PROJECT FINAL REPORT for Korean – AFOSR Nanoscience and Technology Initiative

< Fabrications and Characterizations of $ZnO/Zn_{1-x}Mg_xO$ Nanorod Quantum Structures >

< May 15, 2007>

Name of Principal Investigator: Prof. Gyu-Chul Yi

Institution: Pohang University of Science and Technology (POSTECH)
Mailing address: National CRI Center for Semiconductor Nanorods
Dept. of Materials Science and Engineering,
POSTECH,
San-31 Hyoja-dong
Pohang, Gyeongbuk 790-784
Korea (ROK)
Phone: +82-54-279-2155
FAX: +82-54-279-8635
e-mail address: gcyi@postech.ac.kr

Report Documentation Page

Form Approved
OMB No. 0704-0188

1. REPORT DATE	2. REPORT TYPE	3. DATES COVERED
05 DEC 2007		

4. TITLE AND SUBTITLE	5a. CONTRACT NUMBER
Fabrications and Characterizations of ZnO-based Nanorod Heterostructures III	5b. GRANT NUMBER
	5c. PROGRAM ELEMENT NUMBER

6. AUTHOR(S)	5d. PROJECT NUMBER
Gyu Chul Yi	5e. TASK NUMBER
	5f. WORK UNIT NUMBER

7. PERFORMING ORGANIZATION NAME(S) AND ADDRESS(ES)	8. PERFORMING ORGANIZATION REPORT NUMBER
Pohang Univ. of Science & Technology,San-31 Hyoja-dong,Pohang, Kyungbuk, South Korea,KS,790-784	**N/A**

9. SPONSORING/MONITORING AGENCY NAME(S) AND ADDRESS(ES)	10. SPONSOR/MONITOR'S ACRONYM(S)
	11. SPONSOR/MONITOR'S REPORT NUMBER(S)

12. DISTRIBUTION/AVAILABILITY STATEMENT

Approved for public release; distribution unlimited.

13. SUPPLEMENTARY NOTES

14. ABSTRACT

Semiconductor nanorod heterostructures opens up significant opportunities for fabricating electronic and photonic nanodevices. Especially, semiconductor nanorod quantum structures (QS)s with well-defined interfaces benefit developing nanoscale resonant tunneling devices, field effect transistors, and light-emitting devices. Recently, ZnO/MgxZn1-xO nanorod QSs were fabricated by modulating composition along axial and radial direction. These novel nanorod QSs opened up the possibilities of developing nanoscale photonic systems.

15. SUBJECT TERMS

16. SECURITY CLASSIFICATION OF:			17. LIMITATION OF ABSTRACT	18. NUMBER OF PAGES	19a. NAME OF RESPONSIBLE PERSON
a. REPORT	b. ABSTRACT	c. THIS PAGE			
unclassified	**unclassified**	**unclassified**	**10**	**10**	

Overview

Recent demonstration of semiconductor nanorod heterostructures opens up significant opportunities for fabrication of electronic and photonic nanodevices on single nanorods. The semiconductor nanorod quantum structures with well-defined interfaces are main components for nanoscale resonant tunneling devices, field effect transistors, and light-emitting devices since the nanorod quantum structures (QSs) enable novel physical properties such as quantum confinement and formation of minibands. In particular, for these nanorod quantum structures, spectral wavelength can be tuned by varying the well thickness, and the light emission efficiency is significantly enhanced at room temperature. However, quantum confinement effects in nanowires/nanorod heterostructures have not been easily observed despite recent synthesis of compositionally modulated nanowire superlattices by the vapor–liquid–solid (VLS) growth process. This may result from the relatively broad heterostructure interfaces caused by re-alloying of alternating reactants in the metal catalyst during the condensation-precipitation process. In that case, abrupt interfaces can be obtained using our unique method, a catalyst-free nanorod heteroepitaxial growth technique. This nanorod growth method makes it possible to control the thickness of each layer within the monolayer level by utilizing direct adsorption of atoms on the surface of nanorods. We demonstrated this to be the case by the fabrication of ZnO/MgZnO nanorod QSs which exhibit the clear signature of quantum confinement, an increasing blue shift with decreasing layer thickness. Nevertheless, optical properties of a single semiconductor nanorod quantum structure have rarely been reported. In this research, we investigated luminescent characteristics of a single nanorod QS including ZnO/MgZnO coaxial nanorod single-quantum-wells and ZnO/MgZnO nanorod double-quantum-wells using photoluminescence and cathodoluminescence spectroscopy. In addition, we demonstrated nanophotonic switch based on the coupling behavior between optical near-field and ZnO/MgZnO nanorod double-quantum-wells.

Introduction

Semiconductor nanorod heterostructures opens up significant opportunities for fabrication of electronic and photonic nanodevices on single nanorods. Especially, semiconductor nanorod quantum structures with well-defined interfaces are main components for nanoscale resonant tunneling devices, field effect transistors, and light-emitting devices. Recently, we fabricated $ZnO/Mg_xZn_{1-x}O$ nanorod QSs by composition modulation along axial and radial direction. These novel nanorod QSs opened up the possibilities of fabrication and investigate photonic system in nanoscale.

Further improvement in fabrication of coaxial nanorod SQWs enables observation of reduced thermal quenching behaviors of PL. Although the fabrication of ZnO nanorod QSs has been confirmed by spectral PL results, the optical properties of a single ZnO nanorod QS can be strongly affected by defects and fluctuations of compositions and dimension. Accordingly, a complete understanding of the recombination physics of carriers requires local probe method which can investigate luminescent characteristics of a single nanorod QSs. Cathodoluminescence (CL) spectroscopy of nanorod heterostructures offers a powerful technique to investigate luminescence behavior of quantum structures. In this research, we investigated low temperature CL properties of nanorod QSs.

Meanwhile, nanophotonic integrated circuits will require light emitters, detectors, and signal processing units in nanoscale. ZnO nanostructure is a promising material for realizing nanophotonic devices operating in the wavelength of blue and ultraviolet range. Furthermore, demonstration of semiconductor nanorod quantum-well structure of which dimensions are precisely controlled enables us to fabricate nanometer-scale photonic devices on single nanorods. ZnO/MgZnO nanorod QSs have been fabricated by catalyst-free techniques. In addition, further improvement in the fabrication of nanorod heterostructures has resulted in tuning of band structures in nanorod quantum wells. The precise control method of quantum well dimensions can manipulate the allowed and forbidden band formation. To confirm the engineering of optical properties of individual ZnO QSs for realizing nanophotonic devices, we measured the photoluminescence (PL) spectra from the isolated ZnO nanorod double-quantum-wells (DQWs) using a low temperature near-field optical microscope (NOM). By measuring a series of near-field PL measurements, we demonstrated that the ZnO nanorod DQWs can be utilized as nanophotonic switches.

Results

1. Fabrication and photoluminescent characteristics of ZnO/$Mg_{0.2}Zn_{0.8}O$ coaxial nanorod single quantum well structures

During the last research period, we fabricated ZnO/$Mg_{0.2}Zn_{0.8}O$ coaxial nanorod single-quantum-well structures (SQWs) on Si and Al_2O_3 substrates using catalyst-free metalorganic chemical vapor deposition (MOCVD). Our catalyst-free MOCVD enables us to fabricate the nanorod heterostructures having abrupt and well-defined interfaces with precisely controlled thickness on an angstrom scale without broad intermediate transition layer. The core ZnO nanorods are grown on Si and Al_2O_3 substrates using catalyst-free MOCVD. The subsequent deposition of a $Mg_{0.2}Zn_{0.8}O$ shell layer was *in-situ* performed by addition of *bis*-cyclopentadienyl-Mg (cp_2Mg) as the Mg precursor in the same chamber, resulting in coating a $Mg_{0.2}Zn_{0.8}O$ layer on the entire surfaces of the ZnO nanorod surfaces. The ZnO/$Mg_{0.2}Zn_{0.8}O$ coaxial nanorod quantum structures were prepared by the repeated alternate deposition of ZnO quantum well (QW) and $Mg_{0.2}Zn_{0.8}O$ quantum barrier (QB) layers. In our fabrication method, the average growth rates of the ZnO (QW) and $Mg_{0.2}Zn_{0.8}O$ (QB) shells were roughly 0.25 and 0.33 Å/sec, respectively.

Figure 1 shows 10 K PL spectra of ZnO/$Mg_{0.2}Zn_{0.8}O$ coaxial nanorod single quantum well structures with different well layer widths of 8, 15, and 30 Å. The PL spectra of the ZnO/$Mg_{0.2}Zn_{0.8}O$ coaxial nanorod single quantum well structures exhibited two dominant PL peaks at 3.364 eV, corresponding to excitonic emissions from the ZnO core nanorods ($I_2^{ZnO\ (core)}$), a new PL peak denoted as $I^{ZnO\ (QW)}$ was observed at 3.467, 3.433, and 3.409 eV, depending on the thickness of the ZnO (QW) shell thickness. Such a blue-shift in the PL emission peak can be understood in terms of the facts that a quantum size effect in the core/multishell nanorod heterostructures generates quantized sublevel states and the quantized energy levels increase with a decrease in the embedded ZnO (QW) shell layer width.

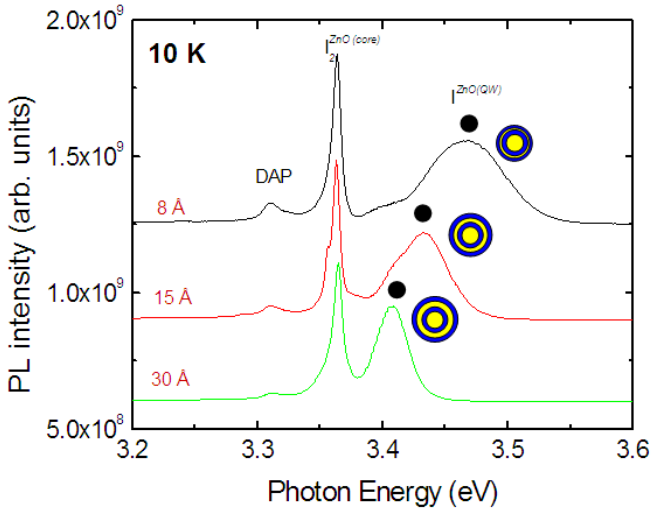

Fig. 1. Low temperature PL spectra of ZnO/$Mg_{0.2}Zn_{0.8}O$ coaxial nanorod quantum structures with various well layer thicknesses (L_W) of 8, 15, and 30 Å.

PL spectra of the coaxial nanorod quantum structures with various QB layer thicknesses were measured to investigate the effect of QB layer thickness on the quantum confinement of the carriers. Figure 2 shows 10 K PL spectra of the coaxial nanorod quantum structures with a ZnO core diameter of 50 nm, a ZnO QW layer thickness of 1.5 nm, and various QB layer thicknesses of 1.5, 3, 6, and 18 nm. For a QB layer thickness of 18 nm, a strong PL peak was observed at 3.427 eV, resulting from the quantum confinement effect in a single ZnO quantum well layer. The intensity of the PL peak decreased significantly with decreasing the QB layer thickness to 6 nm, and then totally disappeared for QB layer thicknesses of 1.5 and 3 nm. This suggests that a QB layer thickness of 6 nm is too thin to confine the carriers or that the QB layers are not uniformly covered with holes present resulting in carrier leakage.

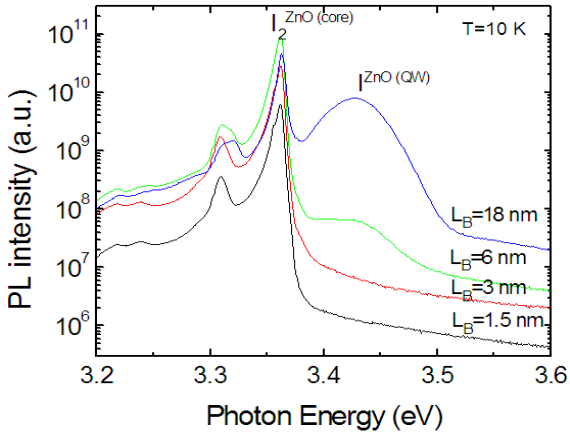

Fig. 2. Low temperature PL spectra of ZnO/$Mg_{0.2}Zn_{0.8}O$ coaxial nanorod quantum structures with various barrier layer thicknesses (L_B) of 1.5, 3, 6, and 18 nm.

Further optical properties of ZnO/$Mg_{0.2}Zn_{0.8}O$ coaxial nanorod quantum structures were investigated by measuring their temperature-dependent PL spectra in the range of 10 and 300 K. Figure 3 shows the temperature-dependent PL spectra of ZnO/$Mg_{0.2}Zn_{0.8}O$ coaxial nanorod quantum structures with an L_W of 15 Å. The two dominant exciton peaks of $I_2^{ZnO(core)}$ and $I^{ZnO(QW)}$ exhibited significant thermal quenching behavior. However, the $I^{ZnO(QW)}$ peak quenched much slowly and survived even at 300 K.

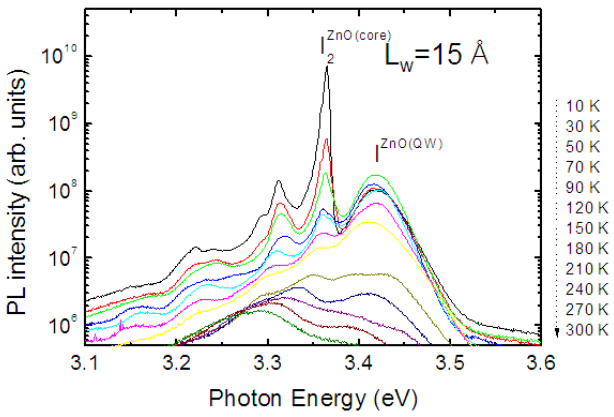

Fig. 3. Temperature-dependent PL spectra of ZnO/$Mg_{0.2}Zn_{0.8}O$ coaxial nanorod quantum structures with L_W of 15 Å

Our controlled growth of ZnO/$Mg_{0.2}Zn_{0.8}O$ coaxial nanorod single quantum well structures opens up significant opportunities for the fabrication of oxide-based quantum device structures with radial composition modulation. These quantum building blocks create well-defined potential profiles along the radial direction in nanorod heterostructures, which would be useful for high electron mobility nanotransistors and light-emitting devices.

2. Cathodoluminescence of single ZnO nanorod heterostructures

The local probing techniques have great potential to investigate the physical properties of nanostructures because their physical properties can be strongly affected by the existence of any fluctuations of dimension and composition. During the last research period, we performed luminescence characterization on individual ZnO nanorod QSs. Here, we report on recent observation on cathodoluminescence (CL) spectra of ZnO/$Mg_{0.2}Zn_{0.8}O$ double-quantum-well structures (DQWs) measured at T = 5 K.

Figure 4 shows the CL spectra of an individual ZnO nanorod DQW with 3.5 nm of the QW width. The CL spectra were measured at different positions along its axis. Although the previous result on ZnO/MgZnO thin film QWs indicated a large red-shifted QW emission due to quantum confinement Stark effect (QCSE), the ZnO nanorod DQW exhibited an emission energy at 3.59 eV higher than that from the thin film QWs. This behavior strongly suggests that the significant QCSE is not observed for the nanorod QWs.

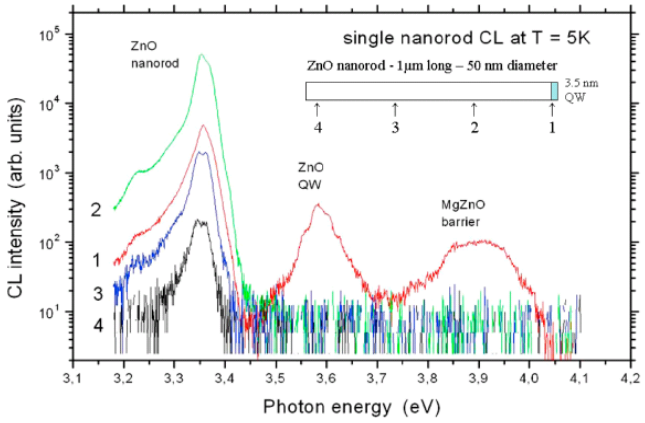

Fig. 4. CL at T = 5 K of a single ZnO nanorod DQW, measured for an electron beam of 15 kV and different locations on the nanorod.

3. A nanophotonic switch using ZnO nanorod double-quantum-wells structures

During the last research period, we demonstrated nanophotonic switch based on optically coupled ZnO/$Mg_{0.2}Zn_{0.8}O$ nanorod double-quantum-well (DQW) structures. To investigate the switching dynamics resulting from controlling the optical near field energy transfer in ZnO nanorod DQW, we performed time-resolved near-field spectroscopy.

The evaluation on the energy transfer in ZnO nanorod DQW was performed on three samples which are depicted in Fig. 5. These ZnO/ZnMgO quantum-well structures (QWs) were fabricated on the ends of ZnO nanorods with a mean diameter of 80 nm using catalyst-free metalorganic vapor phase epitaxy. Figure 6 shows the near-field photoluminescence (NFPL) spectra of ZnO nanorod SQWs, 1-DQWs, and 3-DQWs. Blue-shifted PL peaks were observed at 3.499 (I_S), 3.429 (I_{1D}), and 3.467 (I_{3D}) eV in the far- and near-field PL spectra. These peaks might be originated from the respective ZnO QWs because their energies are comparable to the predicted ZnO well layer thicknesses of 1.7 (I_S), 3.4 (I_{1D}), and 2.2 (I_{3D}) nm, respectively.

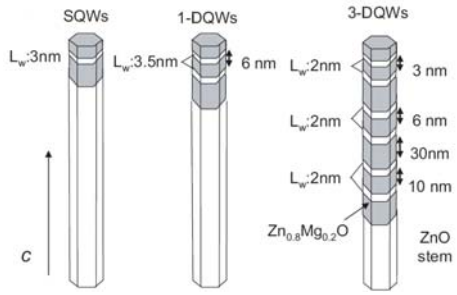

Fig. 5. Schematic of ZnO/ MgZnO SQWs, DQWs (1-DQWs), and triple-pairs of DQWs (3-DQWs).

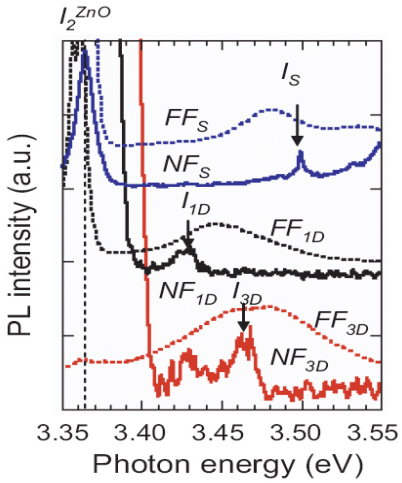

Fig. 6. Near-field time-resolved spectroscopy of ZnO nanorod DQWs at 15 K. (a) *NFS*, *NF1D*, *NF3D*: near-field PL spectra. *FFS*, *FF1D*, *FF3D*: far-field PL spectrum of ZnO SQWs (*Lw* = 2.0 nm), 1-DQWs (*Lw* = 3.5 nm, 6-nm separation), and 3-DQWs (*Lw* = 2.0 nm, 3-, 6-, and 10-nm separation).

To confirm the near-field energy transfer between QWs, we compared the time-resolved near-field PL (TR_{NFPL}) signals at the I_S, I_{1D}, and I_{3D} peaks. According to a three-level system of SQWs, the excitons experience energy transfer between continuum states and excited state when they relax. For DQWs, a similar mechanism can be also applied. However, DQWs experience another process which can be described by coupling between two QW states. Figure 7 shows the numerical results for the exciton population in QWs_1 and the experimental data. In Fig. 8, we observed the faster relaxation for DQWs compared with SQWs and the oscillatory decay. This indicates that the time scale of the near-field coupling is shorter than the decoherence time.

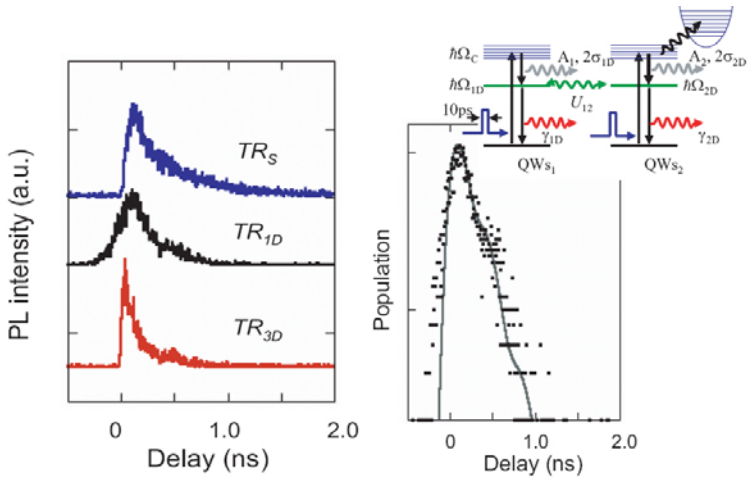

Fig. 7. TR_S, TR_{1D}, and TR_{3D} show TRNFPL signal obtained at I_S, I_{1D}, and I_{3D}, respectively(left). Theoretical results on the transient exciton population dynamics (solid curves) and experimental PL data (filled squares) of 1-DQWs (same as curve TR_{1D}).

Figure 8 shows the separation dependence of the nutation frequencies of 3-DQWs Those of 3-DQWs (PS_{3D}) had three peaks at 1.9, 4.7, and 7.1 ns^{-1}. Since, the degree of the coupling strength, which is proportional to the frequency of the nutation, increases as the separation decreases, the three peaks correspond to the signals from DQWs with separations of 10, 6, and 3 nm, respectively. The exponentially decaying dependence represents that the origin of the peaks in the power spectra from the localized near-field interaction between the QWs.

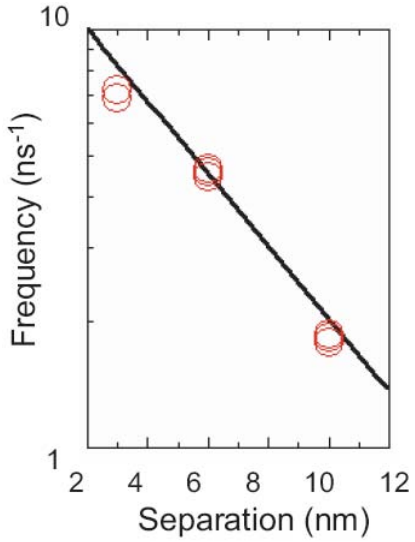

Fig. 8. Evaluation of the nutation frequencies between the QWs. Separation *D* dependence of frequency of the nutation.

We performed the switching operation based on the energy transfer between QW states. Figures 9(a) and (b) show the schemes of the "OFF" and "ON" states based on the DQWs. Assuming L_w = 3.2 and 3.8 nm, the ground exciton state in QW_1 and the first excited state in QW_2 resonate. In the "OFF" operation (Fig. 4(a)), all the exciton energy in QW_1 is transferred to the excited state in the neighboring QW_2 and relaxes rapidly to the ground state. Consequently, no output signals are generated from QW_1. In the "ON" operation (Fig. 9(b)), the escape route to

QW_2 is blocked by the excitation of QW_2 owing to state filling in QW_2 on applying the control signal; therefore, an output signal is generated from QW_1.

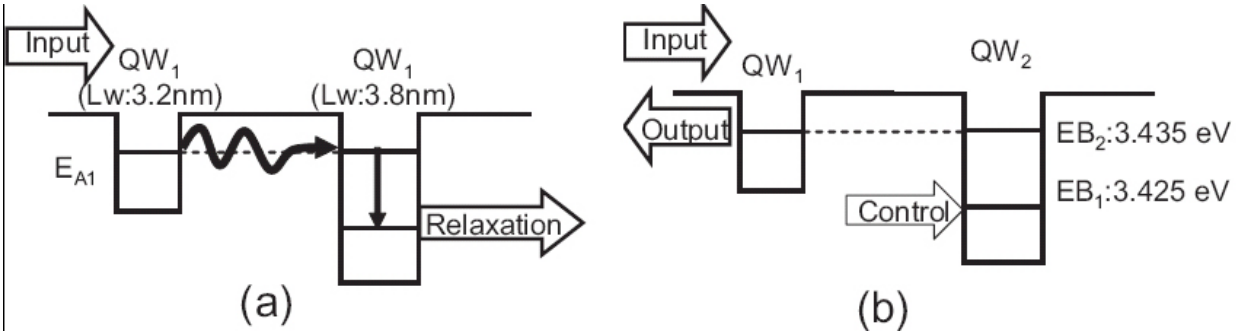

Fig. 9. The switching operation by controlling the exciton excitation. Schematic of the nanophotonic switch of (a) "OFF" state and (b) "ON" state.

Figure 10 shows the NFPL spectra for the three pairs of DQWs with L_w = 3.2 and 3.8 nm with different separations (3, 6, and 10 nm). Curve NF_{OFF} was obtained with continuous input light illumination from a He-Cd laser (3.814 eV). No emission was observed from the exciton ground state of QW_1 (EA_1) or the excited state of QW_2 (EB_2) at a photon energy of 3.435 eV, indicating that the excited energy in QW_1 was transferred to the excited state of QW_2. Furthermore, the excited state of QW_2 is a dipole-forbidden level. Curve $NF_{Control}$ shows the NFPL signal obtained with control light excitation of 3.425-eV with a 10-ps pulse. Emission from the ground state of QW_2 at a photon energy of 3.425 eV was observed. Both input and control light excitation resulted in an output signal with an emission peak at 3.435 eV, in addition to the emission peak at 3.425 eV (curve NF_{ON}), which corresponds to the ground state of QW_2. Since the excited state of QW_2 is a dipole-forbidden level, the observed 3.435-eV emission indicates that the energy transfer from the ground state of QW_1 to the excited state of QW_2 was blocked by the excitation of the ground state of QW_2.

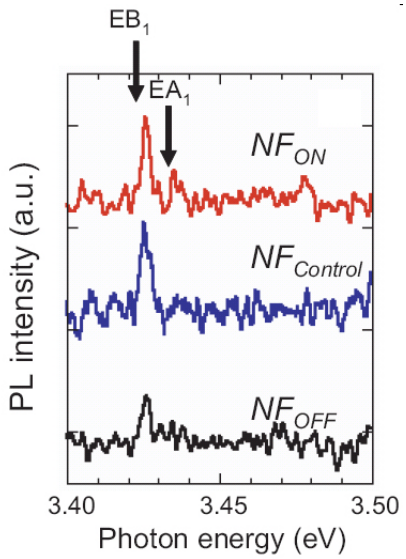

Fig. 10. NF_{ON}, $NF_{Control}$, and NF_{OFF} show NFPL signal obtained with the illumination of Input laser along, Control laser alone, and Input and Control laser, respectively.

In this research, we observed the nutation between DQWs and demonstrated the switching dynamics by controlling the exciton excitation in the QWs. Systems of optically coupled nanorod QWs should be applicable to quantum information processing.

Achievements

Papers:

1. Takashi Yatsui, Suguru Sangu, Tadashi Kawazoe, Motoichi Ohtsu, Sung Jin An, Jinkyoung Yoo, and **Gyu-Chul Yi**, "A nanophotonic switch using ZnO nanorod double-quantum-well structures", Applied Physics Letters (accepted).

2. Bernard Piechal, Jinkyoung Yoo, Abdelhamid Elshaer, Augustine Che Mofor, **Gyu-Chul Yi**, Andrey Bakin, Andreas Waag, Fabrice Donatini, and Le Si Dang, "Cathodoluminescence of single ZnO nanorod heterostructuers", Physica Status Solidi (b), **244**, 1458 (2007).

3. Jun Young Bae, Jinkyoung Yoo, and Gyu-Chul Yi, "Fabrication and photoluminescent characteristics of ZnO/$Mg_{0.2}Zn_{0.8}O$ coaxial nanorod single-quantum-well structures", Applied Physics Letters, **87**, 173114 (2006).

Presentations and proceedings:

1. **Gyu-Chul Yi**, presentation in the 6th Nanoarchitectonics Workshop (2007).

2. **Gyu-Chul Yi**, presentation in UKC (2006).

3. Jinkyoung Yoo, **Gyu-Chul Yi**, Bonghwan Chon, Taiha Joo, Takashi Yatsui, and Motoichi Ohtsu, presentation in the TMS Electronic Materials Conference (2006).

4. **Gyu-Chul Yi**, presentation in Workshop on Electronic and Transport properties of nanomaterials (2006).

5. **Gyu-Chul Yi**, presentation in ICMOVPE-XIII (2006).

6. **Gyu-Chul Yi**, presentation in 3rd US-Korea workshop on Nanoelectronics (2006).

7. Jinkyoung Yoo, Won Il Park, Dong-Wook Kim, and **Gyu-Chul Yi**, presentation in MRS 2006 spring meeting (2006).

8. **Gyu-Chul Yi**, presentation in the 3rd KOREA-US Nano Forum (2006).